FINAL REPORT

Project ID # 86984 Project Title: **Caustic Waste-Soil Weathering Reactions and Their Impacts on Trace Contaminant Migration and Sequestration**

Lead Principal Investigator: Dr. Jon Chorover, Department of Soil, Water and Environmental Science, 429 Shantz Building, University of Arizona, AZ 85721: Tel: (520) 626-5635; Email: chorover@cals.arizona.edu

Co-Investigators: Dr. Karl T. Mueller, Department of Chemistry, 104 Chemistry Building, Penn State University, University Park, PA 16802; Tel: (814) 863-8674; Email: ktm2@psu.edu; Dr. Peggy O'Day, School of Natural Sciences, University of California, Merced, CA 95344; Tel: (209) 724-4338; Fax: (209) 724-2912; E-mail: poday@ucmerced.edu; Mr. R. Jeff Serne, Pacific Northwest National Laboratory, Applied Geology & Geochemistry Group, Richland, WA 99352; Tel: (509) 376-8429; Email: jeff.serne@pnl.gov *Graduate Students*: Garry Crosson, Geoffrey Bowers, Nelson Rivera. *Postdoctoral Scholars*: Sunkyung Choi, Wooyong Um, Aaron Thompson

1. Introduction

The principal goal of this project was to assess the molecular nature and stability of radionuclide (^{137}Cs, ^{90}Sr, and ^{129}I) immobilization during weathering reactions in bulk Hanford sediments and their high surface area clay mineral constituents. We focused on the unique aqueous geochemical conditions that are representative of waste-impacted locations in the Hanford site vadose zone: high ionic strength (*I*), high pH and high Al concentrations. The specific objectives of the work were to (i) measure the coupling of clay mineral weathering and contaminant uptake kinetics of Cs^+, Sr^{2+} and I^-; (ii) determine the molecular structure of contaminant binding sites and their change with weathering time during and after exposure to synthetic tank waste leachate (STWL); (iii) establish the stability of neoformed weathering products and their sequestered contaminants upon exposure of the solids to more "natural" soil solutions (i.e., after removal of the caustic waste source); and (iv) integrate macroscopic, microscopic and spectroscopic data to distinguish labile from non-labile contaminant binding environments, including their dependence on system composition and weathering time. During this funding period, we completed a large set of bench-scale collaborative experiments and product characterization aimed at elucidating the coupling between mineral transformation reactions and contaminant sequestration/stabilization. Our experiments included three representative Hanford sediments: course and fine sediments collected from the Hanford Formation (HC and HF, respectively) and Ringold Silt (RS), in addition to investigations with specimen clay minerals illite, vermiculite, smectite and kaolinite. These experiments combined macroscopic measurements of contaminant uptake and release, mineral transformation, and subsequent neoformed mineral dissolution behavior, with detailed studies of solid phase products using SEM and TEM microscopy, NMR, XAS and FTIR spectroscopy. **Our studies have shown direct coupling between mineral transformation reactions and contaminant sequestration/stabilization.**

2. Summary of Results

Studies of the reactivity of radionuclides (Cs, Sr, I) in STWL with natural sediments and model clays were conducted by coupling macroscopic sorption-desorption experiments with spectroscopic and microscopic investigations over a wide range of reaction times. Three experimental systems were studied: (1) model clay minerals, (2) products of homogeneous precipitation from STWL, and (3) representative Hanford sediments, with (1) and (3) reacted with STWL from 1 h to 369 d. The clay minerals included illite, vermiculite, smectite and kaolinite, which constitute a sequence of micaceous weathering products with variable reactivity toward Cs^+, Sr^{2+} and I^-. Solutions were analyzed by inductively coupled plasma-mass spectrometry (ICP-MS). Solid products (referred to here as "secondary" or "product" phases relative to the initial reactant minerals) were analyzed for time-dependent changes in mineralogy and modes of contaminant bonding by a variety of methods, including X-ray diffraction (XRD), scanning and transmission electron microscopy (SEM and TEM) with energy dispersive spectrometry (EDS), thermogravimetric analysis (TGA), nuclear magnetic resonance (NMR),

X-ray absorption spectroscopy (XAS), including extended X-ray absorption fine structure (EXAFS) and X-ray absorption near-edge structure (XANES) analysis, and Fourier-transform infrared spectroscopy (FTIR).

A. Clay Mineral Systems:

Specimen clays were reacted for times ranging from 1 h to 369 d in batch aqueous systems with a synthetic tank waste leachate (STWL: 2.05 M Na^+, 1.0 M NO_3^-, 0.05 M $Al(OH)_4^-$, and 1.0 M OH^-) in the presence of Cs^+ and Sr^{2+}, where both metals were present as co-contaminants at initial aqueous concentrations ranging from 10^{-5} to 10^{-3} m (all at 298 K). The reactant clays were 2:1 layer-type silicates - illite (Il), vermiculite (Vm) and montmorillonite (Mt) and 1:1 layer-type kaolinite (Kt). Clay mineral type affected the rates of (i) hydroxide promoted dissolution of Si, Al and Fe, (ii) precipitation of secondary solids, and (iii) uptake of Cs and Sr (Chorover et al., 2003; Choi et al., 2005a,b, Crosson et al., 2006). Initial Si release to solution followed the order Mt~Kt > Vm > Il. An abrupt decrease in soluble Si and/or Al after 7 to 33 d for Kt, Mt and Vm systems, and after 190 d for Il suspensions, was concurrent with accumulation of secondary aluminosilicate precipitates. Precipitation resulted in significant removal of STWL Al from solution when parent mineral dissolution was rapid, as was observed for Mt (Chorover et al., 2003; Choi et al., 2005a).

Strontium uptake exceeded that of Cs in both rate and extent, although sorbed Cs was generally more recalcitrant to subsequent desorption and dissolution. After 369 d reaction time, reacted Il, Vm, Mt and Kt solids retained up to 25, 46, 20 and 16 mmol kg^{-1} (0.27, 0.23, 0.03 and 0.69 μmol m^{-2}) of Cs. The fraction of sorbed Cs that was not removed in subsequent ion (Mg^{2+}) exchange or oxalic acid (AAO) dissolution reactions amounted to 70% for Il, 100% for Vm, 20% for Mt and 63% for Kt of the total sorbed mass, indicating a significant pool of strongly retained (or recalcitrant) Cs in all clay mineral systems. After 369 d of reaction time, the same solids sorbed 33 (Il), 47 (Vm), 38 (Mt) and 45 (Kt) mmol kg^{-1} of Sr, of which 0% (Il), 57% (Vm), 58% (Mt) and 87% (Kt) was non-extractable.

Solid Phase Characterizations:

Microscopic and spectroscopic studies were conducted to assess mineral transformation processes in the clay mineral systems. Incongruent clay dissolution resulted in an accumulation of secondary aluminosilicate precipitates identified as nitrate-sodalite, nitrate-cancrinite, chabazite and zeolite X, by molecular spectroscopy and electron microscopy (XRD, IR, NMR, SEM-EDS and TEM-EDS). Contaminant fate was found to be strongly dependent on competing uptake to parent clays and weathering products (Choi et al., 2005b). TEM-EDS results indicated that high Il affinity for Cs was due to adsorption at frayed edge sites. The Il system also comprised Sr-rich aluminous precipitates after 369 d reaction time. In both Kt and Mt systems, Cs and Sr were co-precipitated into increasingly recalcitrant spheroidal precipitates over the course of the experiment, whereas contaminant association with montmorillonite platelets was less prevalent. In contrast, Cs and Sr were found in association with weathered Vm particles despite the formation of spheroidal aluminosilicate precipitates that were similar to those formed from Mt or Kt dissolution.

X-ray Absorption Spectroscopy (XAS):

Bulk and microfocused Sr K-edge EXAFS data were collected to elucidate Sr coordination in reacted clay samples. Reaction progress in the kaolinite system was examined by XAS from 1 to 369 d. Strontium K-edge XAS fluorescence data for bulk samples were collected at the National Synchrotron Light Source (NSLS) on beamline X-18B (2.58 GeV, 300 mA) using an unfocused beam, a Si(111) monochromator crystal, and an Ar-filled Lytle detector. Spectra for two bulk samples (324 d and 369 d-AAO) were collected at the Advanced Photon Source (APS) on GSECARS beamline 13-BM-D with Si(111) monochromator crystal and 16-element Ge fluorescence detector. Microfocused X-ray absorption spectra were collected at the Advanced Photon Source (APS) on GSECARS beamline 13-ID-C with a Si(111) monochromator crystal and a single-element SiLi fluorescence detector. All kaolinite data were collected at room temperature. For the 2-to-1 clays, bulk samples aged for 369 d were analyzed for Sr K-

edge EXAFS at the Stanford Synchrotron Radiation Laboratory (SSRL) on BL11-2 at 4 K using a Si(220) monochromator crystal. Energy for all XAS data was calibrated by setting the mid-point of a $SrCO_3$ reference compound to 16,105 eV.

Analyses of bulk EXAFS spectra in the kaolinite-reacted sampled showed that Sr initially forms a precipitate by 7 d with a local structure similar to $SrCO_3$(s). At 33 d, microfocused EXAFS of individual particles in one sample revealed a mixture of hydrated and dehydrated Sr associated with the neoformed feldspathoid phases. At aging times of 93 d and longer, bulk EXAFS spectra and supporting characterizations indicated the presence of non-exchangeable Sr with a local structure consistent with incorporation into increasingly crystalline aluminosilicate particles, particularly sodalite (Choi et al., 2006). After one year of reaction with STWL for all four clays, the EXAFS data showed that Sr is incorporated into feldspathoid-type phases in kaolinite samples (Choi et al., 2006), is associated mostly with a $SrCO_3$(s) structure in illite samples, and is found in a mixture of $SrCO_3$(s) and feldspathoid or zeolite-type phases in vermiculite and montmorillonite samples (Fig. 1). The feldspathoid phases are indicated by Si/Al backscattering atoms at ~3.46 Å in the kaolinite system. In the case of vermiculite and montmorillonite, Si/Al backscattering atoms are present at distances between ~3.2-3.6 Å, suggesting more variability in the host secondary aluminosilicate phases. The EXAFS spectrum of montmorillonite also indicates scattering of heavy elements (either Sr or Cs) at 4.2-4.9 Å that are interpreted as occupancy of Sr or Cs in adjacent extraframework cation sites. These results show that irreversible Sr incorporation into neoformed aluminosilicate phases is an effective sequestration mechanism for all clay systems except illite, where desorption experiments also show that Sr is easily removed.

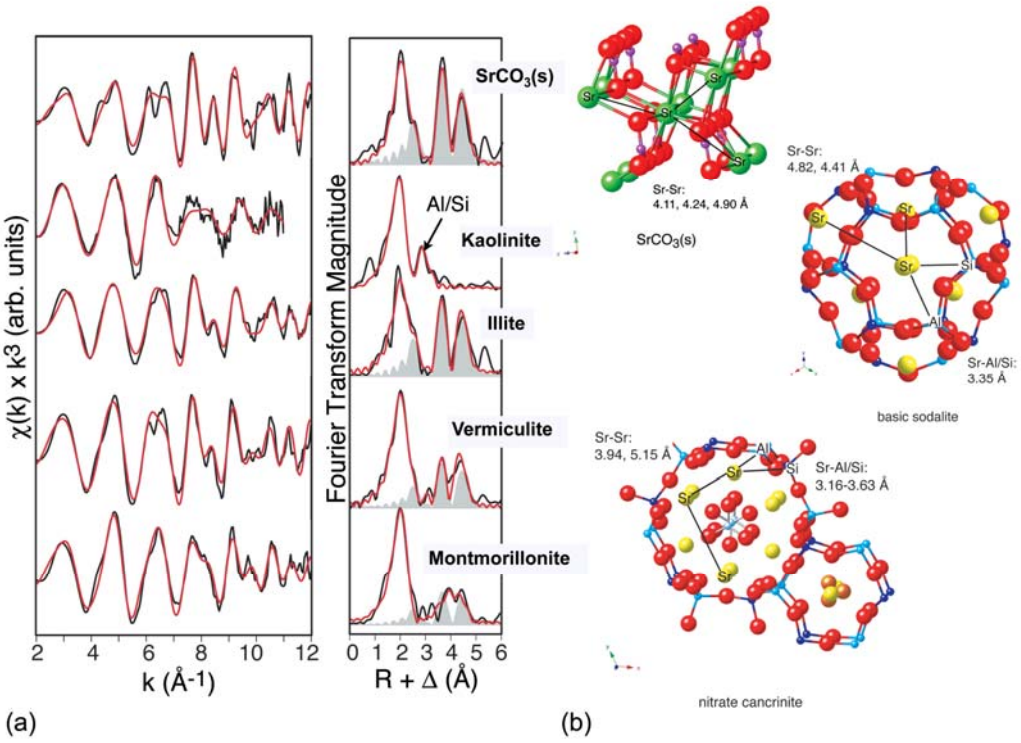

Figure 1. (a) Bulk Sr-EXAFS spectra of reference clays reacted with STWL containing 10^{-3} m Sr and Cs for one year compared to $SrCO_3$(s) reference compound. Black lines are data; red lines are non-linear least squares fits. Shading indicates the fraction of the total EXAFS fit attributed to a $SrCO_3$(s) component at distances greater than first-shell oxygen atoms. (b) Molecular structure models of $SrCO_3$(s), basic sodalite, and nitrate cancrinite showing characteristic interatomic distances between Sr and near-neighbor atoms if Sr was substituted in cation sites in sodalite and cancrinite.

Collectively, these results suggest a reaction progress for Sr that is controlled by the formation of secondary phases and that depends, in turn, on the dissolution and release of rate of Si from the parent clay. In the kaolinite system, uptake of Sr from solution occurs initially by formation of a transient carbonate phase in the presence of ambient CO_2 at alkaline pH. This finding is similar to results from previous experimental studies of Sr adsorption on kaolinite and oxide phases. However, as kaolinite dissolution progresses and more Si is available in solution, Sr is incorporated into nucleating zeolite and feldspathoid minerals. The combination of hydrated and dehydrated Sr in the same sample at 33 d shows a kinetic limitation to the transition from weakly bound, hydrated Sr to more strongly bound dehydrated Sr associated with small, newly formed aluminosilicate particles. At longer reaction times, Sr is primarily dehydrated and non-extractable, and appears to be strongly bound at cation sites in sodalite and/or cancrinite phases. Comparison of the EXAFS spectra to macroscopic behavior of Si and Al release and Sr extractability (Chorover et al., 2003) suggests that the transition into strongly bound sites is a function of total Sr concentration and occurs at earlier times (before 33 d) in experiments with total Sr concentrations of 10^{-4} and 10^{-5} M. At the higher Sr concentrations of the samples probed by EXAFS (10^{-3} M), the formation of a surface carbonate phase early in the reaction progress may contribute to slowing the rate of clay dissolution, which supplies Si for the formation of zeolite and feldspathoid phases. At lower total Sr concentrations, the solubility of $SrCO_3$ was probably not exceeded and the rate of kaolinite dissolution was accelerated (Chorover et al., 2003; Choi et al., 2005a). Further aging of samples indicates that Sr is incorporated into similar types of cation sites in feldspathoid-type phases and undergoes partial dehydration (based on EXAFS interatomic distances), which accounts for its strong bonding.

In the other model clay systems, the rate of Si release from reaction with STWL determines the rate of formation of Sr-sequestering secondary aluminosilicate minerals. In the case of Il after one year of reaction, most Sr is still easily exchanged. Analysis of the Sr EXAFS indicates Sr is associated mostly with $SrCO_3$(s), which is probably present as a poorly crystalline surface coating that is easily dissolved. In the Vm and Mt systems, bulk Sr EXAFS analysis and XRD indicates a mixture of $SrCO_3$(s) and Sr associated with neoformed feldspathoid phases (mostly sodalite and cancrinite), of which the latter are more recalcitrant to chemical extraction. Thus the rate of weathering and Si release correlates directly with the formation of new aluminosilicates that sequester Sr and Cs. In Si-limited systems, there is no apparent kinetic barrier to the precipitation of $SrCO_3$(s) when the solubility of that phase is exceeded; however, removal of Sr from solution by precipitation of $SrCO_3$(s) is readily reversed.

Solid-State NMR:

Solid-state NMR provides molecular-level characterization of local environments for nuclei contained in weathered and reacted aluminosilicate systems, reporting on local bond-order, next-nearest neighbor environments, and molecular- or atomic-level interactions between species. Of interest in our current studies are ^{23}Na, ^{27}Al, ^{29}Si, ^{133}Cs, and ^{87}Sr NMR spectra, which provide details of the structural changes and incorporation of cations into the original and new phases. We have shown each of these nuclei to be useful in characterizing the structure and binding within multicomponent phases, and have embarked on novel studies of, in particular, high-field ^{27}Al MAS NMR spectroscopy and single-resonance ^{87}Sr NMR spectroscopy.

Solid-state NMR spectra have been obtained at a variety of magnetic field strengths using instrumentation both at Penn State University (where fields of strength 7.0 – 11.7 T are available) and within the Environmental Molecular Sciences Laboratory (a national scientific user facility sponsored by the U.S. DOE Office of Biological and Environmental Research) located at the Pacific Northwest National Laboratory (PNNL), operated by Battelle for the DOE. At PNNL, NMR spectrometers were used with magnetic field strengths of 17.6, 18.8, and 21.1 T (corresponding to ^{1}H resonance frequencies of 750, 800, and 900, MHz respectively).

^{29}Si and ^{27}Al magic-angle spinning (MAS) NMR spectroscopy have provided structural and kinetic information in weathered kaolinite and montmorillonite specimen clay systems (Chorover et al., 2003; Choi et al., 2005b; Crosson et al., 2006). By performing MAS NMR experiments at a range of magnetic field strengths, we have extracted full sets of relative populations, isotropic chemical shift

values, and quadrupolar parameters for tetrahedrally coordinated aluminum sites in four new phases formed by the weathering of kaolinite in an STWL for up to 369 days (Crosson et al., 2006). The kinetics of secondary phase formation can then be mapped based on total aluminum speciation or the separate formation kinetics of all four phases (e.g., see Fig. 2a). The data indicate incipient formation of sodalite, followed by transformation to more stable cancrinite, which is consistent with XRD results, but provides more accurate quantitation. Further studies of montmorillonite (Choi et al., 2005b) have provided overall quantitative rates for formation of neophases (Fig. 2b), and work is progressing towards a full kinetic analysis in this system as well (Crosson et al., in preparation).

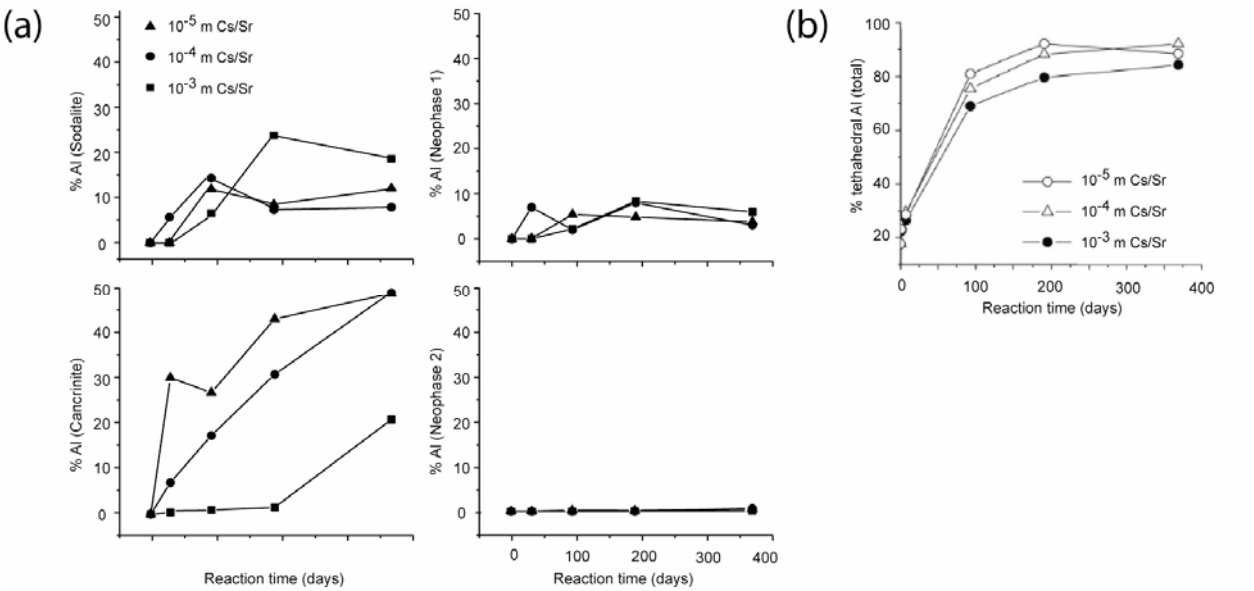

Figure 2. (a) Analysis of quantitative ^{27}Al MAS NMR data at a variety of magnetic field strengths allows a study of the time dependence of formation of four different phases containing four-coordinate aluminum in kaolinite systems reacted for up to 369 days with a STWL solution. (b) Lower-field (7.0 T) ^{27}Al MAS NMR data provide a quantitative tracking of the time dependent formation of neophases in a similarly-weathered montmorillonite system. Complete speciation studies, similar to those performed for kaolinite, are currently being analyzed for accurate quantification of individual phases.

Double-Resonance Determination of Cs Siting in Model Systems

For developing a molecular-scale understanding of contaminant sequestration, double-resonance NMR methods were employed to isolate spectra deriving only from radionuclide-containing neoformed solid phases. ^{29}Si/^{133}Cs double-resonance experiments were first accomplished on a model cesium exchanged sample of chabazite (Crosson, 2005), which is a mineral that is observed to form in STWL impacted clay systems (Chorover et al., 2003). Both Rotational-Echo Double-Resonance (REDOR) and Transfer of Populations via Double-Resonance (TRAPDOR) experiments were successful for indirect detection of the Cs within the pores of the chabazite (see Fig. 3). Initial attempts at ^{29}Si/^{133}Cs double-resonance were also successful in studies of kaolinite after reaction for 190 days with a SWTL containing 10^{-4} m Cs and Sr co-contamination. Additional studies, after an assessment of feasibility of observation of ^{133}Cs signals from these samples, are incorporated into further proposed studies that would include ^{27}Al/^{133}Cs double-resonance as well as possible ^{27}Al/^{87}Sr correlation experiments.

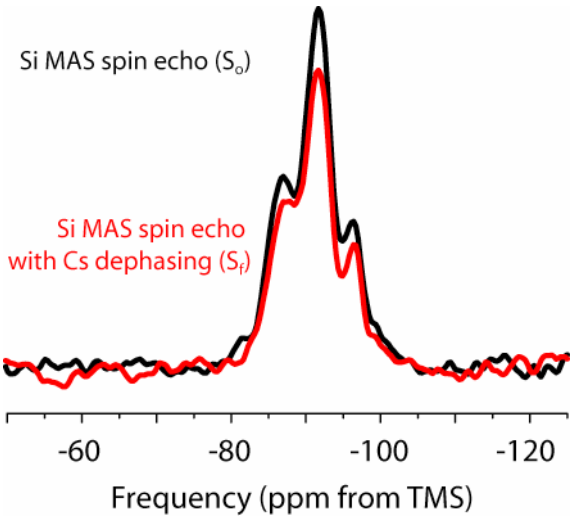

Figure 3. Rotational-Echo Double-Resonance (REDOR) NMR may be used to compare the signals from all Si environments in a complex sample with those Si environments near in space to Cs cations. The difference between the full echo (S_o) and dephased echo (S_f) spectra indicate the spatial proximity of Cs ions to the framework Si species in this sample of chabazite. These experiments are models for our on-going studies of Cs in weathered clay samples.

Dissolution kinetics of Sequestered Sr and Cs:

Contaminant sequestration into solid phase weathering products has important implications for the reactive transport of these constituents in the Hanford vadose zone. Since both Cs and Sr exhibit time-dependent adsorption and incorporation into secondary solids because of HLRW-mineral interactions, it is essential to develop a predictive understanding of contaminant release from mineral solids upon removal of the caustic waste source. Although Cs and Sr uptake into neo-formed solids is favored thermodynamically under conditions of waste-mineral interaction, the fate of these secondary phases and their immobilized contaminants upon re-infiltration of fresh water is not known. To address this need, we reacted illite, vermiculite, montmorillonite and kaolinite for 10 months with STWL and then measured the desorption kinetics of Cs and Sr, as well as dissolution of Si, Al and Fe during reaction with 5 mM $CaCl_2$ solution at pH 8. The contaminant-free $CaCl_2$ solutions were decanted and replenished at regular intervals to prevent solution phase accumulation of Cs, Sr, Al or Si, which would have slowed the mineral dissolution and desorption reactions. The data indicate very little Cs desorption or dissolution from the reacted solids after 40 months, aside from a small initial release at the beginning of the desorption experiment. Although Sr is more readily re-mobilized during the desorption/dissolution reaction, we also observe a large fraction of "sorbed" Sr that is relatively recalcitrant to re-dissolution in the clay systems in which significant mineral transformation has occurred (Kt and Mt). In those systems, 60-80% of the sorbed Sr mass remains immobilized in the solid phase after 40 months of reaction with simulated fresh water. Irreversible "sorption" of Cs and Sr into recalcitrant solids is indicated by immobilization of these contaminants in the solid phase over a desorption timeframe that exceeds that of the uptake reaction by about four times.

Summary:

We have documented a complex time-dependent interplay between mineral transformation and contaminant partitioning in incongruently weathering clay mineral systems (Chorover et al., 2003; Choi et al. 2005a,b; Crosson et al., 2006; Choi et al., 2006). These model studies indicate that parent mineralogy plays a central role in controlling (i) the rate and extent of Cs and Sr sequestration into recalcitrant forms and (ii) the influence of contaminant concentration on mineral transformation rates. The extent to which contaminants are sequestered irreversibly by neoformed aluminosilicate precipitates depends on sorptive

affinity for the parent clay and clay dissolution rate. In the case of Kt and Mt, and to some extent with Vm, rapid dissolution and relatively low concentrations of high-energy sorption sites for Cs and Sr results in the long-term uptake of these contaminants into product feldspathoid phases that form on time scales of weeks to years. Since the rate of clay dissolution at high pH is surface-reaction limited, increased contaminant concentrations and associated sorption of Sr (and possibly Cs) to reactive surface sites apparently reduces the rate of OH^- attack, diminishes the release of Si to solution, and slows the formation of zeolite-type products. Furthermore, high affinity sorption to the parent clay, as occurs in Il and Vm systems even in the presence of STWL, diminishes the accumulation of Cs in neoformed aluminosilicate phases in those systems, as it is found to accumulate on the weathered clay surfaces instead (Choi et al., 2005b). If systems are Si-limited, uptake of Sr from solution by the precipitation of $SrCO_3$(s) occurs readily when phase saturation is exceeded. However, this neoformed carbonate is readily dissolved in undersaturated solutions and does not supply a chemically resistant removal mechanism for Sr.

B. Homogeneous Nucleation Studies

Since our prior work indicated that Si dissolution kinetics and contaminant concentrations were key factors controlling the rate and trajectory of secondary solid phase formation, batch aqueous experiments of synthetic tank waste containing Cs, Sr, and I in the presence of dissolved Si were conducted over a range of molar ratios of Si to Al in order to characterize reaction products formed in the absence of kinetic effects that might arise from the presence of a solid. Synthetic tank waste leachate (STWL) (same as above) was spiked to give three initial aqueous phase Cs^+,Sr^{2+} and I^- concentrations, where individual contaminants (Cs, Sr or I) and co-contaminant mixtures(Cs/Sr. Cs/I, Sr/I and Cs/Sr/I) were added at levels of 10^{-5}, 10^{-4} or 10^{-3} m. The source of soluble Si was 40 % Ludox colloid, which dissolved immediately upon introduction to STWL. Molar ratios of Si to Al were 1:1, 2:1, 10:1 and 20:1. Batch experiments were conducted at 25 and 60°C in sealed polypropylene copolymer (PPCO) bottles for 1 month, at which time solutions were analyzed. Reaction products were centrifuged, washed, and freeze-dried for characterization by XRD, SEM/TEM, FTIR and NMR (Choi et al., in prep.).

Solid Phase Characterization:

At a Si/Al ratio of 1:1, XRD showed a mixture of feldspathoid sodalite ($Na_8(AlSiO_4)_6(NO_3)_2$) and a smaller amount of cancrinite ($Na_8(Al_6Si_6O_{24})(NO_3)_2 \cdot 4H_2O$) as products. At 2:1 Si/Al, NO_3-cancrinite was the primary product. At high Si/Al ratios (20:1 and 10:1), reaction products were primarily zeolite X and amorphous phases (by XRD). There were no significant differences in mineralogy at room temperature and 60°C, and no variations with the contaminant concentration. Results from FTIR were consistent with XRD, showing typical nitrate and fingerprint bands for cancrinite-bearing samples and higher intensities for hydroxyl and water bands for high Si/Al reaction products. Likewise, TEM showed morphological differences as a function of initial Si/Al. Lath-shaped particles, which are typical of synthetic cancrinite, were observed at Si/Al of 2:1 at room temperature and 60°C. Spheroidal phases (~1 µm) with spikes on the particle edge were present at Si/Al = 1:1. At Si/Al ratios of 10:1 and 20:1, extremely fine particles of different sizes were observed that were susceptible to beam damage, suggesting hydrated or unstable phases.

Solid-state NMR Characterization:

To separate the influences of parent minerals on the formation kinetics of neophases, NMR studies of 30-day reacted homogeneous nucleation products with solution molar Si/Al ratios of 20:1, 10:1, 2:1, and 1:1 have been completed. ^{27}Al MAS NMR was performed at three field strengths; 7.0 T and 9.4 T at Penn State and 17.6 T at the PNNL High-Field Magnetic Resonance Facility (HFMRF). In each case, the spectra show that only tetrahedrally coordinated aluminum species are pressnt in the precipitated phases. We also observe that an increasing number of precipitated species are found as the parent solution Si/Al ratio decreases. High-resolution measurements made at 17.61 T demonstrate that the 20:1 Si/Al precipitates contain only a single tetrahedral aluminum peak at a shift of 60.2 ± 0.5 ppm while four distinct resonances were observed in the tetrahedral region for the 2:1 and 1:1 Si/Al samples at this field.

The quadrupolar product (P_q) and isotropic chemical shift values were calculated for each site from the peak shifts at 9.4 T and 17.6 T. Little change in P_q or isotropic shift was observed as a function of contaminant ion concentration, but slight variations in the chemical shift were observed as the contaminant varied from Cs to Sr to I. Quantitative aluminum measurements at PNNL also showed that the ratio of the four precipitated phases does vary as a function of the parent solution Si/Al ratio. These observations are consistent with ^{27}Al MAS NMR of the mineral weathering studies.

Silicon (^{29}Si) MAS NMR measurements were made on the same samples at 7.04 T. In the case of high solution molar Si/Al ratios, multiple silicon peaks were observed spaced at roughly 5 ppm intervals. These spacings are indicative of silicon tetrahedra with varying numbers of nearest neighbor aluminum tetrahedra. The five peaks were clearly resolved in the 20:1 Si/Al samples and the Si/Al ratio of the precipitate phase was calculated to be 1.48 ± 0.03. Aluminum spectra of the 10:1 Si/Al precipitates indicate that two phases are present in this system and the silicon spectra contain a broad peak that covers the entire shift range, making extraction of a unique Si/Al ratio for the overall sample or the individual precipitate species impossible. In the low parent solution Si/Al ratio precipitates, a single silicon peak was present at a shift indicative of silicon tetrahedra with four nearest neighbor aluminum tetrahedra. This means that each of the four precipitated phases has a Si/Al ratio of exactly 1.0. The silicon results for the 2:1 and 1:1 phases are consistent with ^{29}Si MAS NMR spectra collected during the mineral weathering studies. These data support the conclusion that zeolite-type or other fully tetrahedral aluminosilicate phases are produced in STWL weathering environments and they may result from homogenous nucleation in sediment pore fluids.

Measurements were also made on solids derived from 2:1 and 1:1 Si/Al solutions where the homogeneous nucleation experiments were performed at two different reaction temperatures (25 and 60 °C). Only minor variations in peak shift were observed in the aluminum spectra between the two temperatures. No discernable difference was apparent in the silicon spectra. If these two temperatures represent the range of waste temperatures during the various leak events, NMR evidence allows us to suggest that similar neoformed phases are produced during near-field exposure to tank waste regardless of waste temperature.

C. Hanford Sediments

Contaminant weathering studies conducted on the Hanford sediments (Hanford Coarse-HC, Hanford Fine-HF, and Ringold Silt-RS) indicate important similarities and also contrasts with the clay mineral experiments (Chorover et al., 2004; Chorover et al., *in review*). Rates of Si dissolution and re-precipitation with Al followed the order RS > HC > HF. SEM images revealed weathered surfaces of primary minerals (feldspars, quartz and illite) and the formation of crystalline secondary solid phases (including nitrate-cancrinite) after 183 d reaction time. The precipitation of nitrate-bearing secondary minerals was quantified by time-dependent increases in infrared NO_3 stretching absorbances (*ca*. 1400 cm^{-1}) in DRIFT spectra of washed solids. At early reaction times, sorbent affinity (mass basis) for Cs and Sr decreased in the order RS > HF > HC; however, all sediments had similar Sr sorption capacities after several months reaction time. Strontium uptake to all sediments exceeded that of Cs at nearly all reaction times. After 374 d, the total amount of Cs and Sr sorbed in all systems ranged from 15-37% and 80-93% of the initial concentrations, respectively. Although time-dependent trends for Cs uptake were not clearly evident, the fraction of residual Cs increased slightly over time despite fluctuations. Strontium became progressively recalcitrant to desorption after 92 d, suggesting a significant role for Sr coprecipitation in sediments of the Hanford vadose zone, as was observed for the clay mineral systems.

Release of Cs and Sr from sediments weathered in STWL for 10 months was measured at pH 8 in both 10 mM KCl and 5 mM $CaCl_2$ solutions. Initial desorption rates of both contaminants increase with increasing sorbed mass. Kinetic release data for the two contaminants are quite different. Whereas Cs release is accelerated by reaction with K^+, particularly at low loadings, Sr release is enhanced in the presence of Ca^{2+} over the full sorption range. These results are consistent with Cs sorption to frayed edge sites of micaceous minerals at low initial contaminant concentrations (exchangeable only with cation of similar hydration enthalpy and size), and sorption to low affinity sites at higher concentrations. For Sr,

desorption is much more effective in the presence of Ca^{2+}, also suggesting the potential for Sr exchange in zeolite and/or carbonate sites.

Solid Phase Characterization and X-ray Absorption Spectroscopy (XAS):

Samples reacted for 1 to 374 days with initial Cs and Sr concentrations of 10^{-3} m were analyzed at SSRL on BL11-2 for bulk Sr EXAFS and at the Advanced Light Source (ALS) with a microfocused synchrotron beam on BL 10.3.2 for spatially resolved element distribution from X-ray fluorescence (XRF) and microfocused XRD. Samples treated with acid ammonium oxalate at pH~3 (AAO) after 29 and 374 d reaction were also analyzed. For the microfocused XRF and XRD, samples were prepared on adhesive Kapton tape at room temperature. Reacted sediments were also characterized by laboratory XRD, FTIR, SEM/EDS and TEM.

In all three sediments, bulk EXAFS spectra indicated that Sr is incorporated mostly into neoformed aluminosilicate phases (Si/Al backscattering atoms between 3.2 and 3.7 Å) (Choi et al., in prep.). At short reaction times (7 or 33 d), Sr uptake is mostly by incorporation into poorly crystalline, neoformed aluminosilicates and adsorption, rather than by precipitation of $SrCO_3$(s) as seen in the kaolinite system. In HC and HF sediments after one year of reaction, a small fraction of Sr is associated with $SrCO_3$(s), similar to the result found in the model clay systems Mt and Vm, but the majority of Sr is associated with neoformed feldspathoid phases. Synchrotron microfocused X-ray diffraction confirmed the presence of sodalite and cancrinite secondary phases associated with Sr, and showed the persistence of these neoformed aluminosilicates after extraction with acid ammonium oxalate (Fig. 4, Chorover et al., in review). In both unextracted and AAO-extracted HC sediment, micro-XRD patterns showed sodalite and cancrinite associated with Sr-rich areas. In bulk EXAFS spectra after AAO treatment, a fraction of Sr

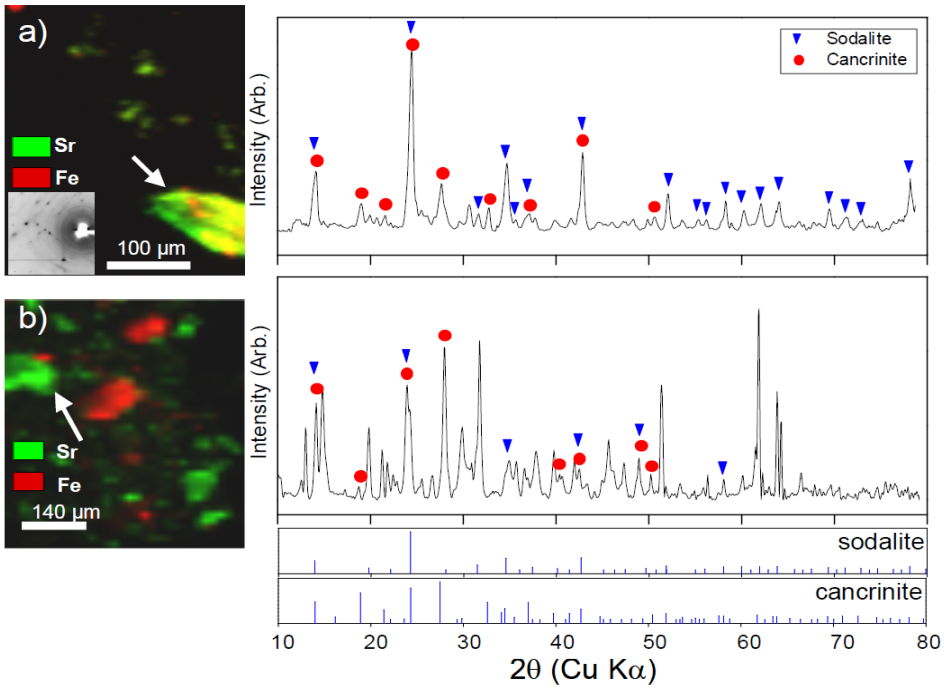

Figure 4. Microfocused synchrotron X-ray fluorescence maps and micro-diffraction patterns of Hanford (WA) soil particles (HC) after reaction for 374 d with caustic synthetic tank waste leachate (top), and the same sample after extraction with acid-ammonium oxalate extraction (bottom). Secondary sodalite and cancrinite that sequestered contaminant Sr formed as products of reaction of leachate with soil minerals. Diffractograms show the persistence of the secondary sodalite and cancrinite phases after extraction treatment, which does not remove sequestered contaminant Sr.

remained bonded in feldspathoid-type structures (Si/Al backscattering at ~3.31 Å), while any carbonate fraction originally present was removed by the extraction. Bulk XRD, FTIR, and SEM/EDS characterizations confirmed the presence of sodalite and cancrinite, in addition to other unidentified zeolite-type phases, associated with Sr and Cs after 182 d to one year of reaction.

Summary:

As in the model clay systems, Sr and Cs incorporation into neoformed aluminosilicate phases is an effective irreversible sequestration mechanism, although the more facile Cs removal suggests preferential incorporation of Sr within cages of neoformed feldspathoids such as sodalite and cancrinite and association of Cs with micaceous minerals in the Hanford sediments (Chorover et al., in review). Unlike the behavior in the kaolinite system, bulk EXAFS spectra of sediments showed that Sr is associated with mostly feldspathoid -type phases or is adsorbed at reaction times of one month or less, and is not precipitated as $SrCO_3$(s). After one year of reaction in the sediments, Sr is present in mixtures of feldspathoid phases, where Sr becomes strongly bound in cation sites and thus resistant to mobilization, and in a small fraction associated with $SrCO_3$(s). These results suggest that Sr uptake by neoformed sodalite and cancrinite appears to be limited by supply of Si from the dissolution of primary phases. Excess Sr not taken up by these feldspathoid phases is either adsorbed on surfaces or precipitated as $SrCO_3$(s), which makes this fraction of Sr more at risk for mobilization if pH or groundwater solution composition changes.

Progress Towards Molecular-Level Characterization of Sr Binding Sites with Solid-State NMR

The coordination environment of Sr is an important indicator of the sequestration of the radioactive nuclides released into the environment. Complimentary to EXAFS and x-ray studies, solid-state NMR studies of ^{87}Sr will provide details of the local environments of the Sr and hence their location in complex reaction product mixtures. However, ^{87}Sr is a very difficult nucleus to detect via NMR for a number of reasons, and hence our research has been focused on fundamental studies of Sr via NMR in order to determine levels of detection as well as the dependence of measurable NMR parameters on local structure. Magic angle spinning (MAS) strontium NMR studies were first performed on simple crystalline compounds. In a study published in *Physical Review B*, we showed that MAS is a very effective tool for analyzing strontium nuclei present in highly symmetric environments. We performed MAS rotor-synchronized echo experiments at 8 kHz and 5 kHz spin rates and used the results to calculate the distribution of electric field gradients (efgs) brought about by point defects in the crystal structures of SrO, $SrCl_2$, and SrF_2. (Bowers and Mueller, 2005) These defects cause local variations in the electric field gradient manifested as a distribution of small quadrupolar coupling constants that can be determined by examination of the spinning sideband pattern. By fitting the integrated sideband intensities to a Lorenztian distribution, one can extract the distribution of efg's within the sample and in principle calculate the total number of defect sites in the materials with near zero efg's about a quadrupolar nucleus. These results show that if strontium is present in a symmetric binding environment, detection and analysis will be straightforward with conventional MAS. However, MAS is difficult to apply effectively for more complicated strontium-containing crystal structures, as the large quadrupole moment of strontium produces broad resonances in the presence of any appreciable electric field gradient. MAS experiments at 9 kHz in an 11.74 T (^1H resonance freq. of 500 MHz) magnet of strontium nitrate and sulfate, both of which posses quadrupolar coupling constants in excess of 10 MHz, have been ineffective at simplifying the spectra or providing additional information beyond that available from static results. The effectiveness of MAS on resonances dominated by the quadrupolar interaction can be improved by both increasing the external magnetic field strength, which results in a reduction of the central transition linewidth, and by increasing the spin rate, which reduces the number of spinning sidebands over which the intensity is dispersed. MAS NMR results from 21.14 T did show an improvement in the effectiveness of MAS NMR on strontium nitrate, but proved ineffective for samples with larger quadrupolar coupling strengths.

We therefore have explored other means to enhance the sensitivity of low-γ quadrupolar nuclei, such as performing quadrupolar Carr-Purcell Meiboom-Gill (QCPMG) experiments at the highest available external magnetic field strength. QCPMG spectra of strontianite ($SrCO_3$) and celestine ($SrSO_4$) are shown in Figure 5. The acquisition of such spectra was facilitated by use of the 21.14 T NMR spectrometer at PNNL's High-Field Magnetic Resonance Facility. The strontium sites in these materials were characterized by extracting the quadrupolar parameters (C_q and η) and isotropic chemical shifts (δ_{iso}) through iterative simulations of the spectra with the SIMPLEX method provided in the SIMPSON solid-state NMR simulation package. These parameters are highly sensitive to local symmetry and electronic structure about the strontium nuclei and therefore provide information related to coordination, bonding, and the identity of neighboring atoms. These data show a strong relationship between the strontium asymmetry parameter and the arrangement of the coordinating oxygen atoms (Bowers et al., 2006a). Work with additional materials and quantum mechanical calculations are in progress to further understand this trend in terms of the full electromagnetic environment. As expected, there was a substantial improvement in the sensitivity of ^{87}Sr NMR measurements made at 21.14 T. Improvements in spectral signal-to-noise (S/N) from the QCPMG sequence reported here results in **up to ten thousand-fold** reductions in experiment time, clearly demonstrating that QCPMG is a promising method for studying strontium resonances in clays, zeolites, and feldspathoids.

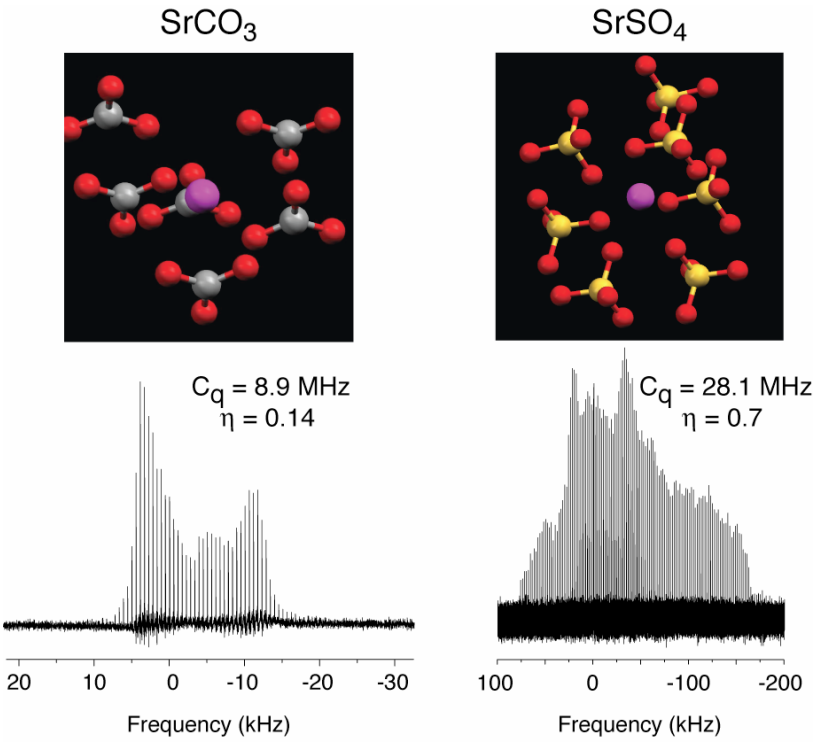

Figure 5. ^{87}Sr QCPMG NMR signals from two model strontium compounds exhibit the strong dependence of quadrupolar interaction parameters (the quadrupolar coupling constant, C_q, and the quadrupolar asymmetry parameter, η) on the local environment of the strontium cations. In the $SrCO_3$ structure, the cation is coordinated by nine oxygen atoms, while in the $SrSO_4$ structure the strontium sits in a highly asymmetric site with twelve neighboring oxygen atoms.

In previous studies, the ability to study strontium nuclei in the homogeneous nucleation systems or weathered clay systems with solid-state NMR was still limited by the low levels of strontium in the samples, although the newer methods described here are designed to overcome these limitations. For more immediate study, we pursued further understanding of the binding environments of strontium in layered aluminosilicate materials. We began with the study of strontium binding in one member of the

swelling mica family (Na-4 mica of nominal composition; $Na_4Mg_6Al_4Si_4O_{20}F_4$) with ^{87}Sr double-frequency sweep (DFS)-QCPMG NMR at 21.14 T (Bowers et al., 2006b). The ^{87}Sr DFS-QCPMG spectrum and best fit analysis are displayed in Figure 6a. From the ^{87}Sr quadrupolar parameters and the *d*-spacing (calculated from XRD), we determined that interlayer strontium is bound in this material as a nine-coordinate electrostatic complex deep in the di-trigonal cavities, where a large electron density is available. However, the interlayer of strontium-saturated Na-4 mica is known to contain both sodium and strontium: our collaborators have shown that the strontium exchange capacity of Na-4 mica is typically 47% of the maximum cation exchange capacity. In such a situation, a near total collapse of the interlayer upon heating may also force some of the residual sodium into the di-trigonal cavities. To fully understand the below-theoretical strontium exchange and active binding mechanisms in this material, it was necessary to identify the binding environment(s) of both the strontium and the residual sodium cations.

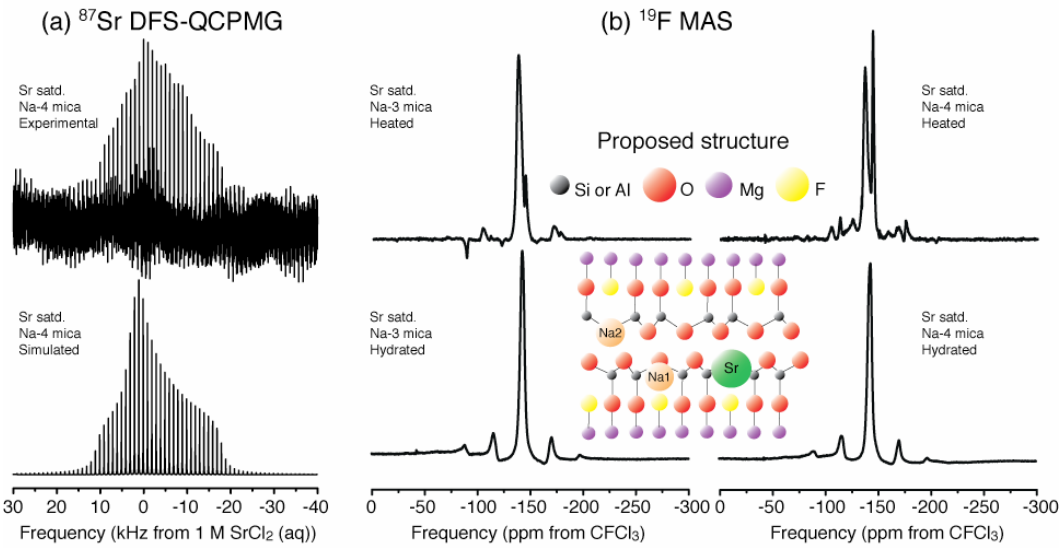

Figure 6. (a) Experimental and simulated ^{87}Sr DFS-QCPMG NMR signals indicate quadruploar parameters of C_q = 9.02 MHz and η = 1.0 for strontium incorporated into a mica designed for environmental remediation of strontium. (b) The ^{19}F MAS NMR spectra of two different micas with strontium absorbed into the interlayer indicate that, upon heating, the local environment of the fluorine atoms becomes perturbed, and we attribute this to the siting of strontium and sodium cations within the structure.

Therefore, in further studies (Bowers et al., 2006c), we combined high-field ^{87}Sr NMR with ^{19}F and ^{23}Na MAS NMR to characterize all interlayer cation environments in two strontium-saturated members of the swelling mica family (the Na-4 mica described above, and a Na-3 mica of nominal composition $Na_3Mg_6Al_3Si_5O_{20}F_4$). NMR experiments were performed on the materials before and after a heat-induced collapse of the interlayer space. In both micas, a new ^{19}F resonance with a peak shift of roughly +5 ppm appears following heat treatment that is associated with fluorine from the octahedral sheet with a nearest neighbor cation bound in the di-trigonal cavity (see Figure 6b). A comparison of the ^{19}F peak integrals indicates that the number of cation-occupied cavities cannot be accounted for by purely strontium or sodium sorption in either mica. The ^{23}Na MAS NMR results indicate the presence of two unique interlayer sodium environments before and after heating, with an additional peak appearing after heat treatment and layer collapse. Elemental analysis and ^{87}Sr NMR suggest that nearly all strontium in the heated micas is bound in the di-trigonal cavities and that the third sodium peak represents residual sodium also bound in the cavities. The remaining sodium is present in the small interlayer space associated with the di-trigonal holes of vacant cavities, or associated with contaminant phases. This combined set of NMR measurements, aided by x-ray diffraction and thermal analysis, provides an atomic-

level view of the binding interactions of strontium in complex aluminosilicate systems, and is a model for our future analyses of weathered aluminosilicate materials.

Peer-Reviewed Publications by Project Principal Investigators

Bostick, B., A. Vairavamurthy, K. G. Karthikeyan, and J. Chorover. 2002. Cesium adsorption on clay minerals: An EXAFS spectroscopic investigation. *Environ. Sci. Technol*. **36**, 2670-2676.

Bowers, G. M. and K. T. Mueller. 2005. Electric field gradient distributions about strontium nuclei in cubic and octahedrally symmetric crystal systems. *Phys. Rev. B* **71**, 224112/1-224112/7.

Bowers, G. M., A. S. Lipton, and K. T. Mueller, 2006a. High-field QCPMG NMR of strontium nuclei in natural minerals. *Solid-State NMR* **29**, 95-103.

Bowers, G. M., M. C. Davis, R. Ravella, S. Komarneni, and K. T. Mueller, 2006c. Cation replacement mechanisms and binding environments in strontium-saturated fluoromicas. Submitted to *Environ. Sci. Technol*.

Bowers, G. M., R. Ravella, S. Komarneni, and K. T. Mueller, 2006b. NMR study of strontium binding by a micaceous mineral. *J. Phys. Chem. B* **110**, 7159-7164.

Choi, S., G. Crosson, K. T. Mueller, S. Seraphin and J. Chorover. 2005b. Clay mineral weathering and contaminant dynamics in a caustic aqueous system. II. Mineral transformation and microscale partitioning. *Geochim. Cosmochim. Acta*. **69**, 4437-4451.

Choi, S., M. K. Amistadi and J. Chorover. 2005a. Clay mineral weathering and contaminant dynamics in a caustic aqueous system. I. Wet Chemistry and Aging Effects *Geochim. Cosmochim. Acta*. **69**, 4425-4436.

Choi, S., P. A. O'Day, N. A. Rivera, K. T. Mueller, M. Vairavamurthy, S. Seraphin, and J. Chorover. 2006. Strontium speciation during reaction of kaolinite with simulated tank-waste leachate: Bulk and microfocused EXAFS analysis, *Environ. Sci. Technol*. **40**, 2608-2614.

Chorover, J., P. A. Rotenberg and R. J. Serne. 2004. Mineral formation and radionuclide sorption in waste-impacted Hanford sediments. In R. B. Wanty and R. R. Seal II (eds.) *Water-Rock Interaction*, pp. 675-678. A. A. Balkema Publishers, Leiden.

Chorover, J., S. Choi, M. K. Amistadi, K.G. Karthikeyan, G. Crosson, and K.T. Mueller. 2003. Linking cesium and strontium uptake to kaolinite weathering in simulated tank waste leachate. *Environ. Sci. Technol.* **37**, 2200-2208.

Chorover, J., S. Choi, P. A. Rotenberg, R. J. Serne, and P. A. O'Day (in review) Coupling contaminant sorption and mineral transformation in Hanford sediments, submitted to *Geochim. Cosmochim. Acta*.

Crosson, G., S. Choi, J. Chorover, M. K. Amistadi, P. A. O'Day and K. T. Mueller. 2006. Solid-state NMR identification and quantification of newly-formed aluminosilicate phases in weathered kaolinite systems. *J. Phys. Chem. B* **110**, 723-732.

Um, W., and R. J. Serne. 2005. Sorption and transport behavior of radionuclides in the proposed low-level radioactive waste facility at the Hanford Site, Washington. *Radiochim. Acta* **93**, 57-63.

Um, W., R. J. Serne, and K. M. Krupka. 2004. Linearity and reversibility of iodide adsorption on sediments from Hanford, Washington under water saturated conditions. *Water Research* **38**, 2009-2016.

Um, W., R. J. Serne, S. B. Yabusaki, and A. T. Owen. 2005. Enhanced radionuclide immobilization and flow path modifications by dissolution and secondary precipitates. *J. Environ. Quality* **34**, 1404-1414.

Wan, J., T. K. Tokunaga, J. T. Larsen, and R. J. Serne. 2004. Geochemical evolution of highly alkaline and saline tank waste plumes during seepage through vadose zone sediments. *Geochim. Cosmochim. Acta* **68**, 491-502.

Publications in preparation:

Choi, S., J. Chorover, N. A. Rivera, C. Strepka, , K. T. Mueller, and P. A. O'Day, Mineral transformation and strontium sequestration from reaction of model clays and Hanford sediments with caustic waste: Molecular characterization.

Choi, S., G. M. Bowers, M. K. Amistadi, K. T. Mueller, P. A. O'Day, and J. Chorover, Cesium, strontium and iodine incorporation and diffusion into zeolite-type phases during homogeneous nucleation at pH 13.

Chorover, J., and M. K. Amistadi. Dissolution kinetics of contaminant-bearing clay mineral weathering products.

Crosson, G. S, G. M. Bowers, C. Strepka, M. K. Amistadi, P. A. O'Day, J. Chorover, and K. T. Mueller, Solid-state NMR identification and quantification of newly-formed aluminosilicate phases in weathered montmorillonite systems.

Theses

Crosson, G., 2005. *Solid-state nuclear magnetic resonance studies of hydroxide promoted dissolution of layered silicates.* Ph.D. Thesis, Penn State University, Department of Chemistry (Mueller-Major Advisor).

Rotenberg, P. A., 2002. *Cesium and strontium uptake and mineral weathering of Hanford Sediments in the presence of a highly alkaline tank waste*. M.S. Thesis in Soil Science, Penn State University (Chorover-Major Advisor).

Bowers, G. M., 2006. *Structural investigation of strontium in inorganic crystals, organic crystals, and phyllosilicate minerals with ^{87}Sr NMR*. Ph.D. Thesis, Penn State University, Department of Chemistry (Mueller-Major Advisor).